EVALUATION OF HYDROGEN PRODUCTION USING CATHENA-ELOCA DURING A LOCA/LOECC SCENARIO

G. Sabourin, G. Parent* and H.M. Huynh*

Atomic Energy of Canada Limited, 1000 rue de la Gauchetière Ouest #1440, Montréal, Québec, Canada H3B 4W5
*Hydro-Québec, 1000 rue de la Gauchetière Ouest, #1400, Montréal, Québec, Canada, H3B 4W5

SUMMARY

A 20% RIH break with loss of ECC and boiler crash cooldown is simulated with CATHENA-ELOCA and CATHENA to assess the fuel and pressure tube temperatures as well as the hydrogen production. Six representative channels are selected to represent six power groups of channels for each core pass. The maximum temperature predicted (1446 ºC for the central element sheath of bundle 6 in channel O6 of the broken pass – 5 g/s) is largely lower than those shown in the 2002 Gentilly-2 Safety Report. The total amount of predicted hydrogen produced is also much lower than the values shown in the 2002 Gentilly-2 Safety Report.

1.0 Introduction

This paper documents single channel analyses performed with CATHENA [1] and CATHENA-ELOCA for a 20% RIH4 break with a total loss of ECC when the burnup distribution in the channel is such that bundles 6 and 7 are at 90 MWh/kg. The 95 channels in the broken and intact passes of the broken loop are represented by 6 single channels. During the post-blowdown phase of the transient, constant steam flowrate of 0, 5, 10 or 100 g/s are considered.

An innovative methodology has been introduced to simulate the blowdown phase of the transient by coupling the CATHENA-ELOCA code, which allows calculating at each time step the gap heat transfer coefficient [2]. Furthermore, a new approach has been introduced for simulating without interruption the blowdown and post-blowdown phases of the transient [3]. The present analysis is based on the same approach documented in [3] although the coupling of CATHENA and ELOCA is now through the software PVM (Parallel Virtual Machine). Details of this coupling are explained in another paper submitted to the 27th Annual Conference of the CNS [4].

The outputs of the simulations are the fuel and fuel channel temperatures as well as the hydrogen production from zircaloy water reaction in the fuel sheaths and pressure tube. The hydrogen production is calculated under two assumptions:

- A constant steam flowrate of 5 g/s in both passes of the broken loop;
- A constant steam flowrate of 5 g/s in the broken pass combined with a constant steam flowrate of 0 g/s (or no flow) in the intact pass.

2.0 Methodology and Assumptions

The methodology used in this analysis of single channels during a postulated 20% RIH4 break with total loss of ECC is shown in Figure 1. The 95 channels of each pass of the

broken loop are represented by 6 single channels: B10, G05, L03, O06, S10 and W10 as shown in Table 1. A 37-element bundle is shown in Figure 2.

2.1 CATHENA Steady States

Headers conditions calculated by SOPHT-G2 (pressure, average fluid enthalpy, void fraction) are converted to give the boundary conditions necessary for CATHENA (pressure, gas phase enthalpy, liquid phase enthalpy, void fraction)

The results of the CATHENA steady states are used as boundary conditions for ELESTRES calculations of initial conditions. The following parameters are given for one element per ring per bundle:

- Coolant temperature,
- Pressure,
- Heat transfer coefficient between the coolant and the sheath.

CATHENA, because it is coupled with ELOCA, needs the heated length, which is a new entry in the CATHENA input file. This entry is necessary in GENHTP because the actual heated length in ELOCA is different from the element length in CATHENA.

2.2 ELESTRES calculations

ELESTRES calculations are performed to produce initial conditions for the coupled CATHENA-ELOCA calculations. ELESTRES produces 'eldat' files that are used by ELOCA. Furthermore, the heated length, the radial dimensions and the radial power distribution of each element are used by CATHENA as initial conditions in the transient simulations.

2.3 CATHENA-ELOCA Transients (Blowdown)

The CATHENA and ELOCA codes are coupled through the PVM program [4]. The coupled program is used to perform the detailed calculations of temperature and hydraulic conditions in each single channel for the blowdown portion of the transient. The transient thermalhydraulic boundary conditions at headers 4 and 1 (pressure, enthalpies, void fraction) for CATHENA come from SOPHT-G2 transient simulation for the 20% RIH4 break with failure of the ECC injection. The pressure boundary conditions in outlet header 1 and inlet header 4 are shown in Figure 3. CATHENA and ELOCA exchange data at each time step.

The coupled calculations give two parameters that will be used in the subsequent independent CATHENA transient calculation: the flowrate at the inlet feeder and the gap heat transfer coefficient for each element of each bundle.

2.4 CATHENA Transients (Blowdown and Post-Blowdown)

CATHENA is used to perform detailed temperature calculations and hydraulic conditions in the channels for a 5000 seconds transient. The hydrogen source term is determined in the same transient analysis. The initial conditions used are the same as those of the coupled calculation. The transient boundary conditions come from SOPHT-G2 results (for the pressure, enthalpy and void fraction at the outlet header) and from CATHENA-ELOCA (for the flowrate in/out of the inlet header). For the first 262 seconds after the break, a flowrate boundary condition is imposed at the inlet header using the flowrate calculated in the coupled transient as discussed in section 2.3. After 300 seconds, a

constant steam flowrate (0, 5, 10 or 100 g/s) is imposed until the end of the transient. For the broken pass, the constant steam flowrate boundary condition is negative, since the flow is toward the break in the inlet header. A linear transition is made on the flowrate boundary condition between 262 and 300 seconds. The temperature of the steam is a boundary condition from the SOPHT-G2 simulation. After 262 seconds it is fixed at a constant value, which is slightly superheated.

The transient gap heat transfer coefficients calculated by ELOCA as discussed in section 2.3, are used by CATHENA for the first 262 seconds of the transient. After 262 seconds, the gap heat transfer coefficient values are assumed constant at their values at 262 seconds.

2.5 Modelling

Each bundle is modelled with 19 cylinders in CATHENA, i.e. with a vertical symmetry. The top element of each ring is modelled by ELOCA in the coupled calculations. The pressure tube and the calandria tube are divided into 12 circumferential sectors. The thermal radiation between the elements and the pressure tube as well as between the pressure tube and the calandria tube is modelled.

2.6 Main Assumptions

The default CATHENA correlations are used, except as discussed below.

Pressure tube deformation with eventual contact with the calandria tube is modelled. CATHENA assumes that the pressure tube retains its circular shape. When contact with the calandria tube by ballooning is predicted, it is assumed to occur on the whole circumference. The ballooning contact conductance is assumed to be 2.5 $kW/m^2/°C$. This value corresponds to the long-term contact conductance between the pressure tube and the calandria tube. At the time of initial contact, the conductance is higher at 11.0 $kW/m^2/°C$., but very rapidly, the pressure tube cools down and the contact is not as good, which has the effect of reducing the conductance to 2.5 $kW/m^2/°C$. For our calculations, it is the long-term conductance that is important, as long as there is no dryout on the calandria tube.

Contact by sag is modelled and assumed to occur for the bottom 60° of both tubes when the pressure tube temperature is higher than 850 °C. The sag contact conductance is assumed to be 6.5 $kW/m^2/°C$. This value is inferred from full-scale contact experiments.

Two radii are used for the calandria tube in the present analysis. The nominal radius of 0.0645 m is used for the coupled calculations during the blowdown phase of the transient. A higher inside radius of 0.0731 m is used during the 5000 seconds transients. This larger radius takes into account the fact that the contacts by sag happen during the blowdown phase and after that, the distance between the top of the pressure tube and the calandria tube is higher than initially.

The decay power is from the ANS 5.1 data shown in the Gentilly-2 Safety Report (Reference [5], Figure I-30).

The moderator subcooling is shown in Table 2.

For the Zircaloy-steam reaction, the Urbanic-Heidric correlation is used [6].

3.0 Results of the 20% RIH Break with Loss of ECC with a Constant Vapour Flow of 5 g/s

The temperature predictions for the 20% RIH break with loss of ECC injectin and crash cooldown, assuming a constant steam flowrate of 5 g/s during the post-blowdown phase of the transient are presented below.

3.1 Base Case, Channel O6 in the Broken Pass

Results for channel O6, which is a high-power channel, are presented first. Channel O6, and O17 have the same geometry but are located in different core passes. For simplicity, both of these channels are called O6. For example, channel O6 of the broken pass is in reality channel O17.

3.1.1 Steady State

The steady state is used to produce boundary conditions for ELESTRES. Table 3 shows these boundary conditions. The last three columns are the fluid temperature in °C, the pressure in kPa(a) and the gap heat transfer coefficient in $kW/m^2/°C$.

3.1.2 CATHENA-ELOCA Results

CATHENA-ELOCA was run for 262 seconds after the break. Figure 4 shows the bundle 6 sheath temperatures and the temperature of the pressure tube at that location for the first 100 seconds of the transient. Detailed results will be discussed in section 3.1.3. Figure 5 shows the gap heat transfer coefficient of the outer ring top element; the break initiation is at 200 s. This gap heat transfer coefficient is calculated by ELOCA using boundary conditions from CATHENA at each time step. In steady state, the gap heat transfer coefficient is about 17 $kW/m^2/°C$ (during the first 200 s). During the power pulse, it increases to almost 40 $kW/m^2/°C$, and decreases near the end of the transient to a value just above 0.3 $kW/m^2/°C$. This low value is due to the channel blowdown and to the large quantity of gaseous fission products in the gap.

3.1.3 CATHENA Results for 5000 Seconds

Figure 6 shows the sheath temperatures of bundle 6. As expected, during the power pulse, the temperatures of the outer ring elements (which have a higher power than the elements in other rings) are much higher than those of the other rings. On the other hand, during the constant steam flowrate phase, the temperature of the central element approaches that of the other elements and eventually becomes higher. This is due to the fact that during this phase, the heat is almost completely transferred by thermal radiation from the elements (especially the outer fuel pins) to the pressure tube and from the pressure tube to the calandria tube.

Figure 7 shows the sheath temperature of the central elements of bundles 6 to 8. During the power pulse the sheath temperatures increase very rapidly. After this, they increase steadily until the power transferred through thermal radiation to the pressure tube is equal to the decay power. The maximum temperature is reached for bundle 6 at 1446.2 °C. The temperatures then start to go down because of the decrease in power until the pressure tube balloons into contact with the calandria tube, showing an abrupt drop in temperatures to the 900 °C range.

Figure 8 and Figure 9 shows the pressure tube top and bottom sectors temperatures for bundle 6, 7 and 8. Table 4 shows the time of contact by ballooning and sag, as well as the heatup rate at each segment of channel O6. The pressure tube contacts the calandria tube by sag from bundle 2 to bundle 10. The pressure tube around bundles 1, 11 and 12 does not reach 850 °C during the transient. Contact occurs by sag before it occurs by ballooning for bundles 6, 7 and 8.

Contact by ballooning occurs after the temperatures have reached their maximum. In the CATHENA simulations, the heatup rate can be negative because of the thermal radiation between the pressure tube and the calandria tube. To evaluate the calandria tube integrity following contact by ballooning, we use the criteria proposed by J. Luxat in [7]. As a conservative assumption, we have used the heatup rate of the pressure tube between 400 and 600 °C (or equivalently between 215 and 250 seconds). With a moderator subcooling of 23.6 °C for channel O6, there is a large margin to prolonged dryout without rewet, according to Figure 15 of [7].

From Figure 10 to Figure 14, we can see the evolution of the axial temperature distribution in the elements and the pressure tube at different times after the end of the blowdown (100 seconds after the break).

3.2 The Other Channels of the Broken Pass

Figure 15 shows the comparison between central element sheath temperatures of all channels of the broken pass. The highest temperature is reached in channel O6. We see that there is an important decrease in sheath temperatures only for channels O6, S10 and L03. These are the channels with the highest powers and it is only in these channels that there is contact by ballooning at bundle 6. Consequently the temperatures in channels B10, G05 and W10 are higher at the end of the transient even though the power in these channels is smaller than the other channels. Figure 16 shows the comparison between pressure tube temperatures of all channels of the broken pass. We see again that only channels O6, S10 and L03 contact the calandria tube by ballooning.

3.3 The Intact Pass of the Broken Loop

Figure 17 shows the comparison between the central element sheath temperatures of bundle 6 in channel 06 using 5 g/s steam flow for each of both passes. The sheath temperatures in the intact pass decrease to a much lower value after the power pulse because there is a complete rewet of the channel in the intact pass. After the start of the constant steam flowrate the temperatures follow generally the same trend as those of the broken pass. There is no ballooning contact in the intact pass, which explains the higher temperatures at the end of the transient.

4.0 Sensitivity Results on the Constant Steam Flowrate

Figure 18 shows the maximum fuel temperature versus the steam flowrate in each channel of the broken pass. Figure 19 shows the comparison of central elements sheath temperatures of bundle 6 of channel O6 for different steam flowrates. The temperatures for the 5 g/s and 10 g/s flowrates are very similar. The temperatures for the 10 g/s flowrate are slightly lower because of the better heat transfer caused by the increased flow. This better heat transfer is more pronounced for the 100 g/s flowrate. In this case, the temperatures do not reach 1000 °C. In the case of 0 g/s, the exothermic reaction

between the zirconium and vapour is rapidly exhausted because of the lack of available oxygen, which decreases the heat production in comparison to the 5 or 10 g/s cases.

5.0 Hydrogen Production

Hydrogen production (or hydrogen source term) is an integrated value over all channels of both passes. The hydrogen production of one channel is multiplied by the number of channels it represents (see Table 1) and this production is added to the production of the other channels of the same pass as well as to that of the other pass.

The hydrogen production depends strongly on the assumed constant steam flowrate. Figure 20 shows the total hydrogen production (in kg) for different flowrates. The total mass of hydrogen produced is almost equal for 5 and 10 g/s, but slightly higher in the 5 g/s case. For the 0 g/s case, the hydrogen production stops early in the transient. For the 100 g/s case, the hydrogen production continues longer but stays under 0.05 kg at the end of the transient. Detailed results for the 5 g/s case in the broken pass are presented in Figure 21. Channel O6 initially produces the highest quantity of hydrogen because its fuel sheath temperatures are the highest. It is eventually exceeded by channel S10 because there are fewer contacts between the pressure tube and the calandria tube in channel S10.

The hydrogen source term is maximum if we assume that all channels of the broken loop have a constant steam flowrate of 5 g/s in the post-blowdown phase. We could also assume that only the broken pass receives a flowrate of 5 g/s, the intact pass having a flowrate of 0 g/s (which is equivalent to saying that the ECC valves are not leaking for the intact pass). The hydrogen source term, in this case, is the sum of the broken pass hydrogen production at 5 g/s, plus the intact pass hydrogen production at 0 g/s. Figure 22 compares the hydrogen source term of the case 5 g/s in both passes (5g/s –5g/s) to the case 5 g/s in the broken pass and 0 g/s in the intact pass (5g/s – 0g/s). As the hydrogen production is much lower in the 0 g/s case, the source term is reduced by 41%.

6.0 Conclusions

The maximum pressure tube and fuel sheath temperatures for 6 channels of each pass of the broken loop have been simulated with CATHENA-ELOCA for a 20% RIH4 break with total loss of ECC. The hydrogen source term for this scenario has also been predicted.

The maximum temperatures predicted in the present analysis (1446.2 °C for the central element sheath of bundle 6 of channel O6 of the broken loop at 5 g/s) are largely lower than those shown in the 2002 Edition of the Gentilly-2 Safety Report. This is due to a number of factors, mainly:

- The use of CATHENA-ELOCA for a more realistic representation of the bundle from the point of view of thermal radiation and gap heat transfer than was allowed by CHAN;
- The constant steam flowrate phase is modelled more realistically. In the present analysis it starts at 262 seconds after the break when the flowrates predicted by the circuit calculations are low and the void fraction is high. In the previous analysis of the Safety Report, the constant steam flowrate phase started 40 seconds after the break.

The total amount of hydrogen predicted in the present analysis is also largely lower than

the values stated in the 2002 Safety Report. As the amount of hydrogen produced depends on the sheath and pressure tube temperatures, it is normal that largely lower temperatures lead to a largely lower hydrogen production. The amount of hydrogen produced is several times (5 times for the case 5 – 0 g/s or 2.5 times for the case 5 – 5 g/s) lower than that stated in the 2002 G2 Safety Report.

Because of this much lower amount of hydrogen produced, the risk of detonation in the containment is nonexistent.

REFERENCES

1. B.N. Hanna, 1998, "CATHENA: A Thermalhydraulic Code for CANDU Analysis", Nuclear Engineering and Design, Vol. 180 (2), pp. 113-131.
2. G. Sabourin and H.M. Huynh, "Approaches to Simulate Channel and Fuel Behaviour using CATHENA and ELOCA", Proceedings of the 17th Annual Conference of the Canadian Nuclear Society, Fredericton, New Brunswick, June 9-12, 1996.
3. G. Sabourin and H.M. Huynh, "Analysis of LOCA/LOECC with a Non-Stop CATHENA Simulation", Proceedings of the 18th Annual Conference of the Canadian Nuclear Society, Toronto, Ontario, June 8-11, 1997.
4. A. Vasić, B.N. Hanna, G.M. Waddington, G. Sabourin and R. Girard, "Linking CATHENA with Other Computer Codes Through a Remote Process", submitted to the 27th Annual Conference of the Canadian Nuclear Society, Toronto, Ontario, June 11-14, 2006.
5. Centrale Nucléaire Gentilly-2, "Rapport de Sûreté, Partie 3: Analyse des Accidents Volume 1", Hydro-Québec, 2002.
6. Urbanic, V.F. and T.R. Heidrick, 1978, High-temperature oxidation of Zircaloy-2 and Zircaloy-4 in steam, Atomic Energy of Canada Report, AECL-6149.
7. J.C. Luxat, "Mechanistic Modeling of Heat Transfer Processes Governing Pressure Tube- To-Calandria Tube Contact and Fuel Channel Failure", Proceedings of the 23rd Annual Conference of the Canadian Nuclear Society, Toronto, Ontario, June 2-5, 2002.

Table 1 Single Channel Powers for the broken pass

	Single Channels					
	O06	**S10**	**L03**	**G05**	**B10**	**W10**
Nb of channels	**2**	**9**	**37**	**16**	**14**	**17**
Power range (MW)	**7.0-7.3**	**6.6-7.0**	**6.0-6.6**	**5.0-6.0**	**4.0-5.0**	**≤ 4.0**

Table 2 Moderator Subcooling

Single Channel	Row of the highest channel of the group	Moderator saturation temperature	Local moderator temperature	Moderator subcooling
		°C	°C	°C
B10	B	104.1	83.1	21.0
G05	C	104.7	83.1	21.6
L03	D	105.4	82.9	22.5
O06	E	106.0	82.4	23.6
S10	E	106.0	82.4	23.6
W10	A	103.4	82.6	20.8

Table 3 ELESTRES Boundary Conditions – Channel O6 – Broken Pass

grappe	anneau	xeq	tempf	tempg	tsatf	tsatg	Tparoi	flux total	**tfl**	**press**	**heq**
			°C	°C	°C	°C	°C	W/m2	**°C**	**kPa**	**kW/m2/°C**
1	centre	-0.240	264	318	318	318	266	157000	**264**	**10940**	**60.9**
	interne	-0.240	264	318	318	318	266	165000	**264**	**10940**	**60.9**
	median	-0.240	264	318	318	318	267	189000	**264**	**10940**	**60.8**
	externe	-0.240	264	318	318	318	267	232000	**264**	**10940**	**60.9**
2	centre	-0.223	267	317	318	318	274	399000	**267**	**10890**	**61.2**
	interne	-0.223	267	317	318	318	274	422000	**267**	**10890**	**61.2**
	median	-0.223	267	317	318	318	275	484000	**267**	**10890**	**61.2**
	externe	-0.223	267	317	318	318	277	596000	**267**	**10890**	**61.2**
3	centre	-0.199	273	317	318	318	283	619000	**273**	**10830**	**61.7**
	interne	-0.199	273	317	318	318	283	656000	**273**	**10830**	**61.7**
	median	-0.199	273	317	318	318	285	750000	**273**	**10830**	**61.7**
	externe	-0.199	273	317	318	318	288	924000	**273**	**10830**	**61.7**
4	centre	-0.171	279	317	317	317	291	730000	**279**	**10780**	**62.2**
	interne	-0.171	279	317	317	317	291	773000	**279**	**10780**	**62.3**
	median	-0.171	279	317	317	317	293	883000	**279**	**10780**	**62.2**
	externe	-0.171	279	317	317	317	296	1086000	**279**	**10780**	**62.3**
5	centre	-0.138	286	316	317	317	300	867000	**286**	**10720**	**63.0**
	interne	-0.138	286	316	317	317	301	917000	**286**	**10720**	**63.0**
	median	-0.138	286	316	317	317	303	1045000	**286**	**10720**	**63.0**
	externe	-0.138	286	316	317	317	307	1283000	**286**	**10720**	**63.0**
6	centre	-0.104	294	316	316	316	309	927000	**294**	**10660**	**63.9**
	interne	-0.104	294	316	316	316	309	980000	**294**	**10660**	**63.9**
	median	-0.104	294	316	316	316	312	1116000	**294**	**10660**	**63.9**
	externe	-0.104	294	316	316	316	315	1367000	**294**	**10660**	**63.9**
7	centre	-0.069	301	315	316	316	316	927000	**301**	**10600**	**64.8**
	interne	-0.069	301	315	316	316	317	980000	**301**	**10600**	**64.8**
	median	-0.069	301	315	316	316	319	1116000	**301**	**10600**	**65.2**
	externe	-0.069	301	315	316	316	322	1367000	**301**	**10600**	**66.4**
8	centre	-0.037	308	315	316	316	321	868000	**308**	**10540**	**67.7**
	interne	-0.037	308	315	316	316	322	918000	**308**	**10540**	**68.1**
	median	-0.037	308	315	316	316	323	1046000	**308**	**10540**	**69.1**
	externe	-0.037	308	315	316	316	326	1284000	**308**	**10540**	**71.1**
9	centre	-0.011	313	315	315	315	323	699000	**313**	**10480**	**71.2**
	interne	-0.011	313	315	315	315	323	738000	**313**	**10480**	**71.6**
	median	-0.011	313	315	315	315	324	838000	**313**	**10480**	**72.6**
	externe	-0.011	313	315	315	315	326	1024000	**313**	**10480**	**74.4**
10	centre	0.010	316	314	315	315	323	582000	**315**	**10420**	**67.6**
	interne	0.010	316	314	315	315	324	612000	**315**	**10420**	**68.1**
	median	0.010	316	314	315	315	325	689000	**315**	**10420**	**69.5**
	externe	0.010	316	314	315	315	326	836000	**315**	**10420**	**71.8**
11	centre	0.025	315	314	314	314	321	396000	**314**	**10360**	**59.5**
	interne	0.025	315	314	314	314	321	416000	**314**	**10360**	**60.2**
	median	0.025	315	314	314	314	322	466000	**314**	**10360**	**61.8**
	externe	0.025	315	314	314	314	323	563000	**314**	**10360**	**64.3**
12	centre	0.032	315	313	314	314	317	160000	**314**	**10280**	**51.3**
	interne	0.032	315	313	314	314	317	168000	**314**	**10280**	**52.1**
	median	0.032	315	313	314	314	317	188000	**314**	**10280**	**53.7**
	externe	0.032	315	313	314	314	318	228000	**314**	**10280**	**56.4**

Table 4 Contacts between the pressure tube and the calandria tube – channel O6 – broken pass – 5 g/s

Ballooning Contact				
Bundle Position	Time	Pressure tube temperature	Applied Pressure (int.-ext.)	Heating rate*
	Seconds	°C	MPa	°C/s
7	1116.6	1196.0	0.129	7.0
6	1327.5	1157.4	0.129	5.4
8	1466.9	1107.5	0.129	5.9

Contact by sag	
Bundle Position	Time
	Seconds
7	397.0
6	402.7
8	406.9
5	426.1
9	464.7
4	484.9
3	577.2
10	584.8
2	844.8

* Average heating rate when the pressure tube temperature increases from 400 to 600 °C

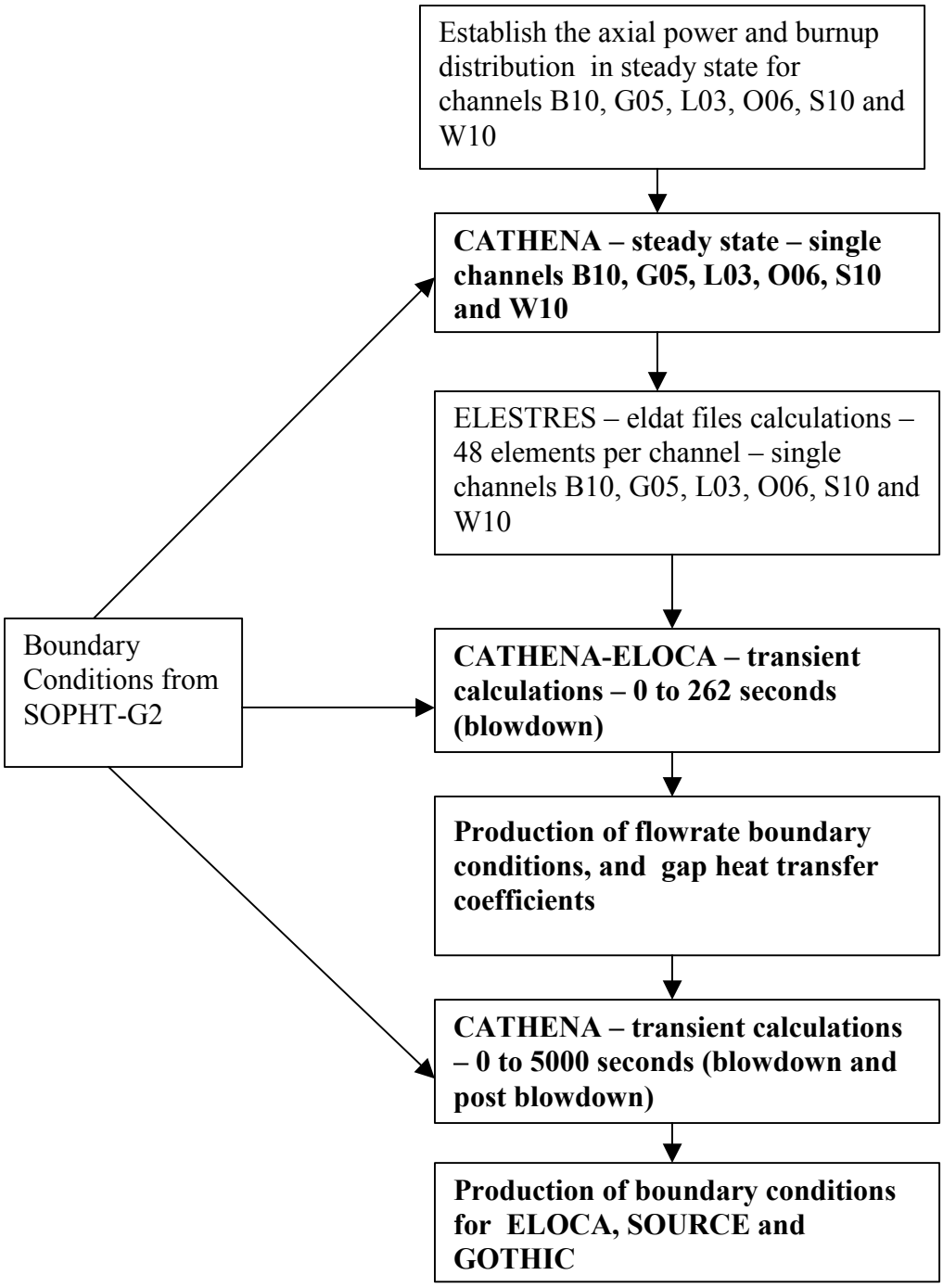

Figure 1: Methodology for CATHENA and CATHENA-ELOCA calculations with single channels.

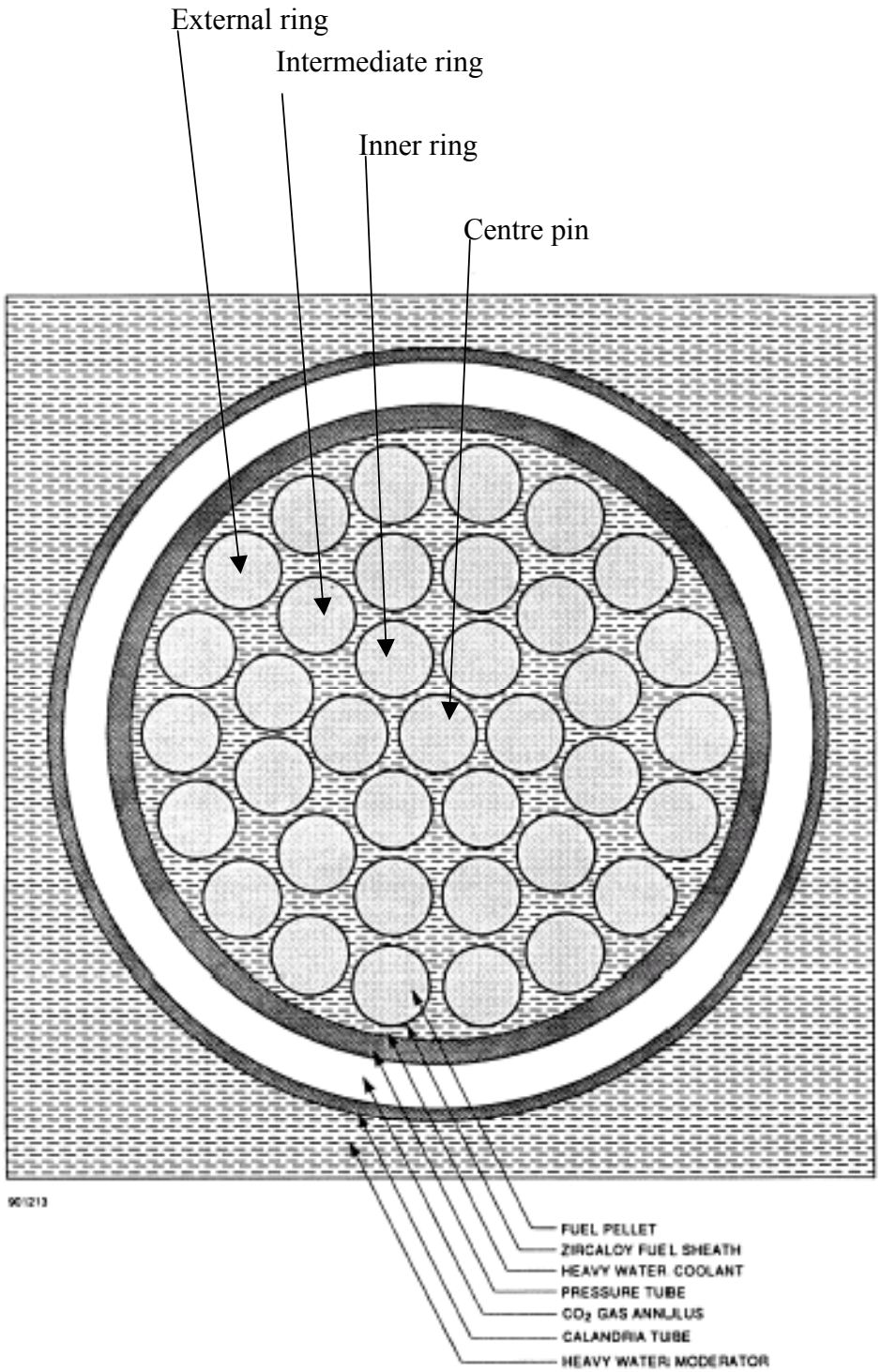

Figure 2 A 37-element bundle

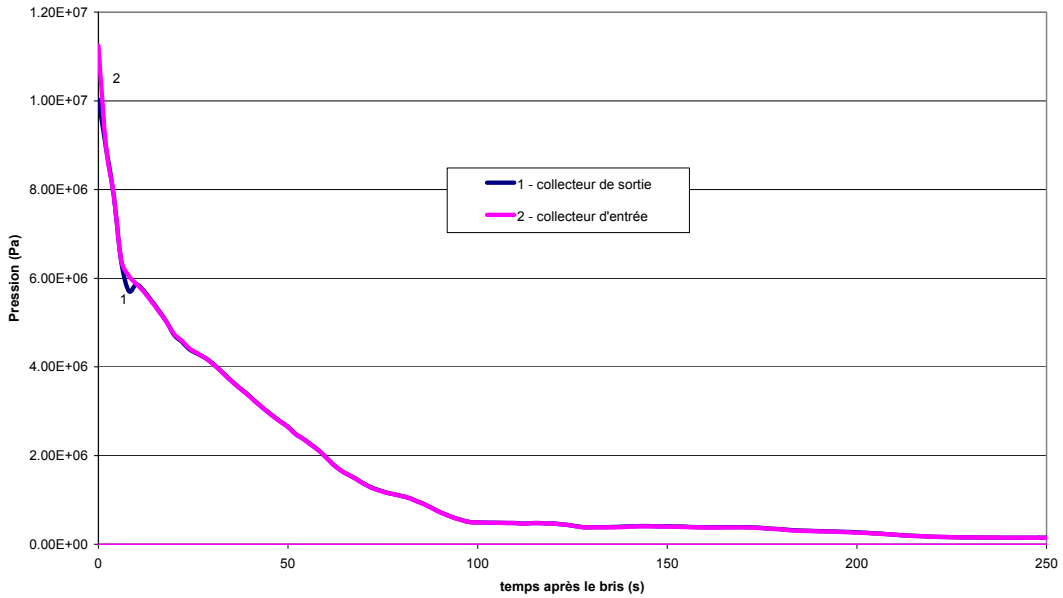

Figure 3 Pressure boundary conditions for the inlet and outlet headers – SOPHT-G2 – 20% RIH4 break with total loss of ECC

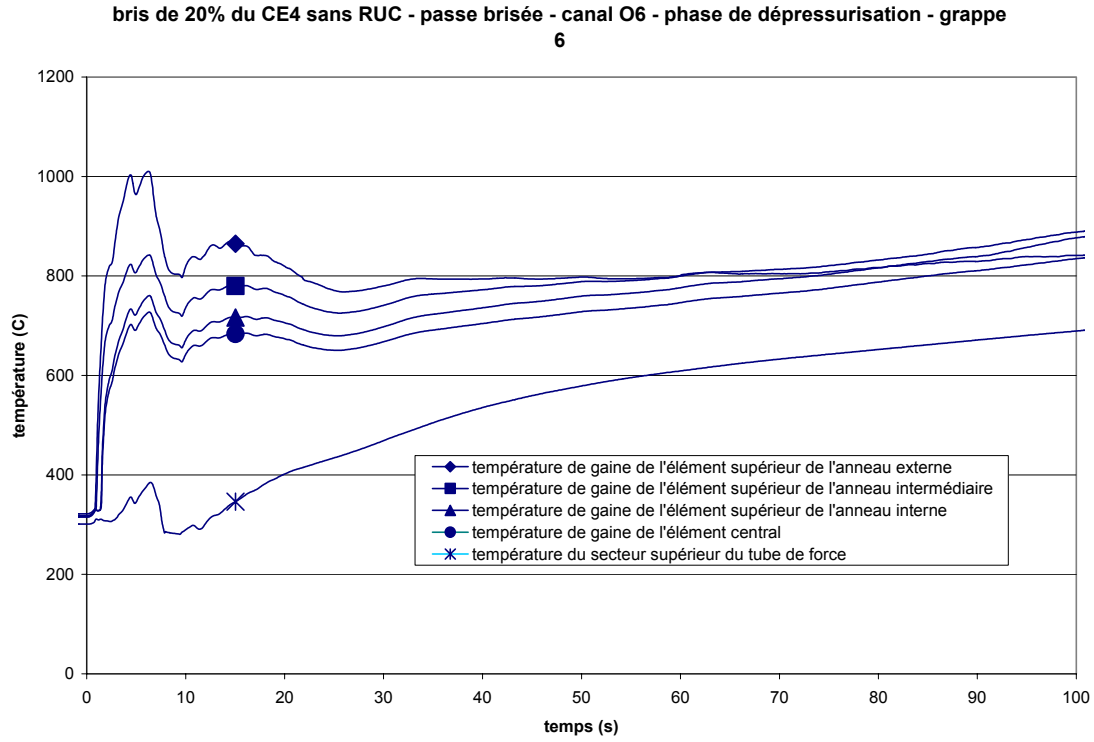

Figure 4 Bundle 6 sheath and pressure tube temperatures for the blowdown phase – channel O6 – broken pass.

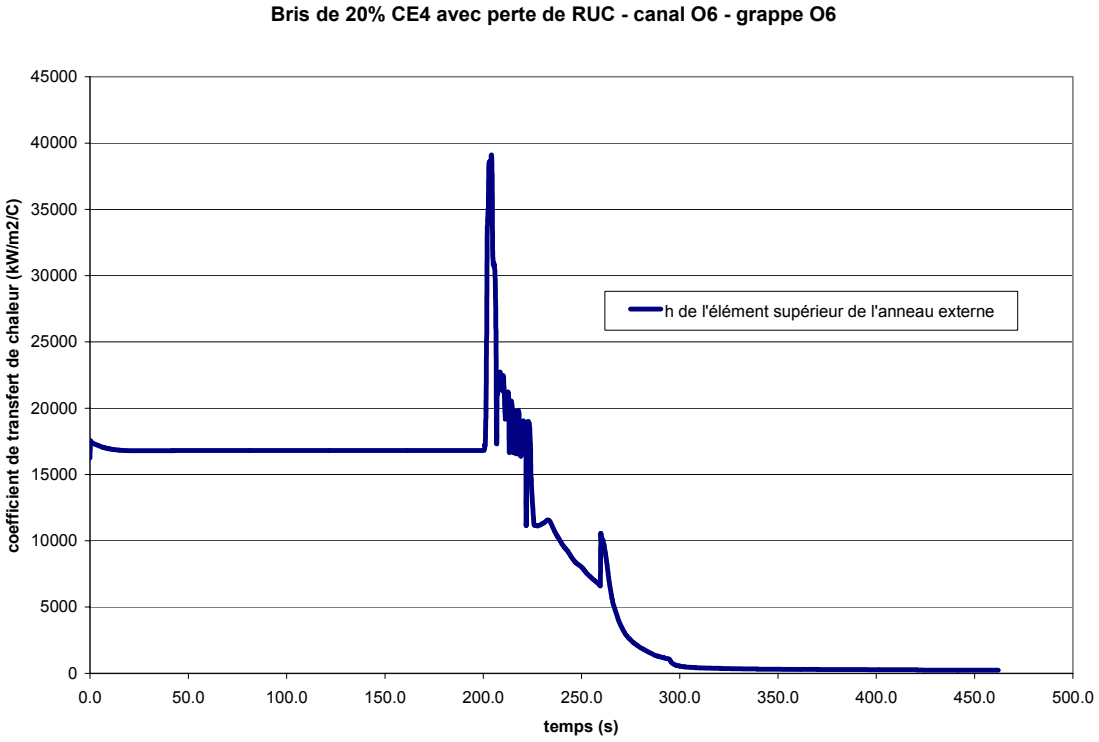

Figure 5 Gap heat transfer coefficient of the outer ring top element of channel O6 bundle 6, predicted by CATHENA-ELOCA.

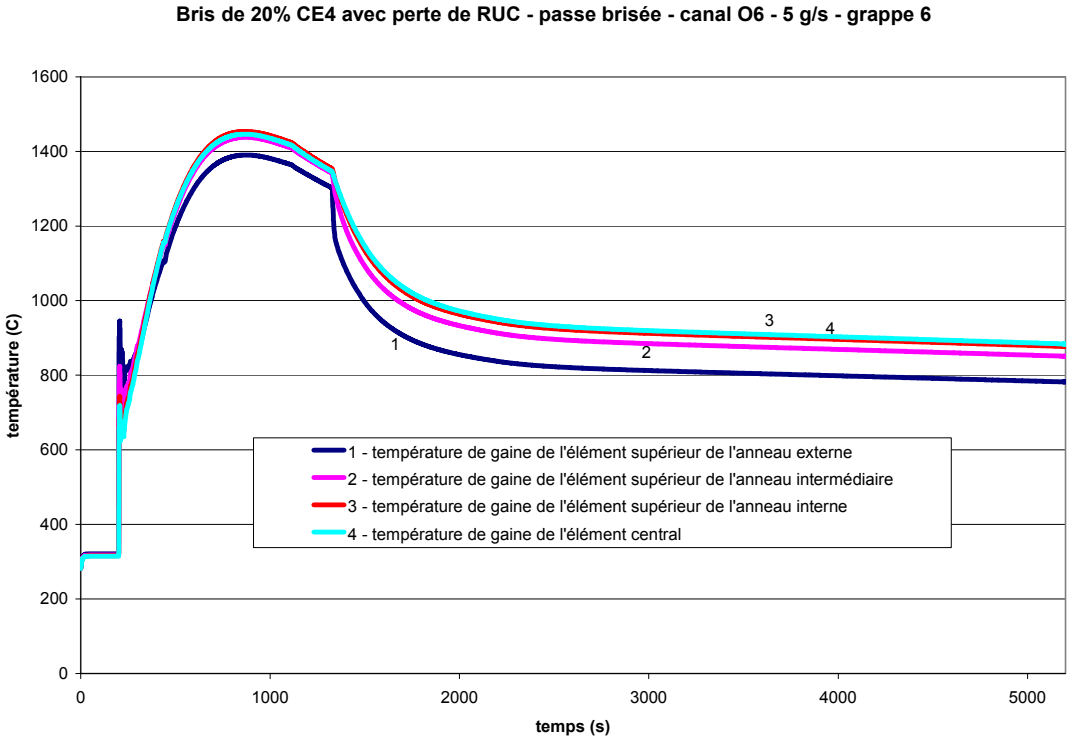

Figure 6 Bundle 6 sheath temperatures – channel O6 – broken pass – 5 g/s.

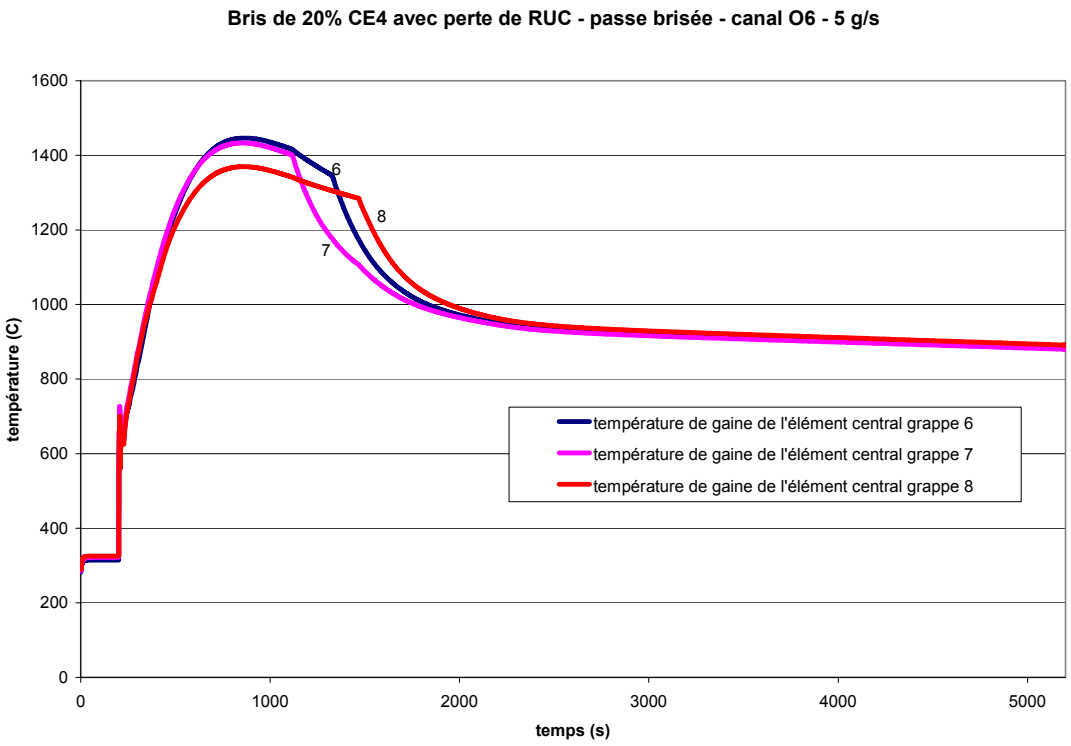

Figure 7 Central elements sheath temperatures – channel O6 – 5 g/s.

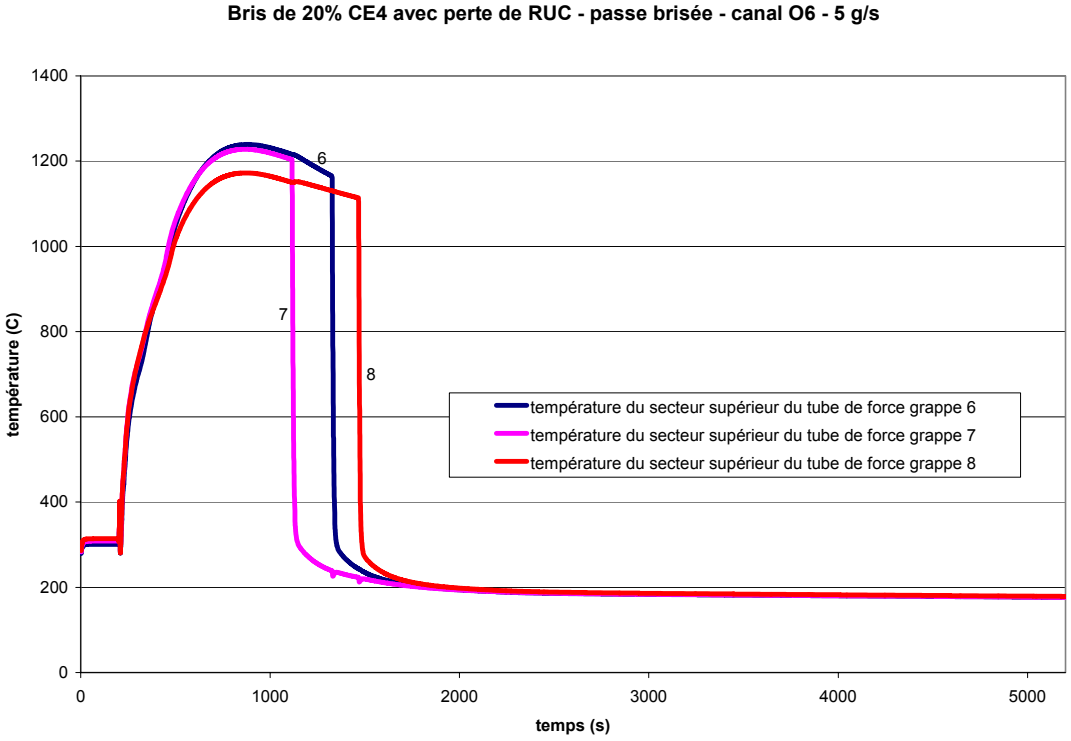

Figure 8 Pressure tube top sector temperatures – channel O6 – 5 g/s

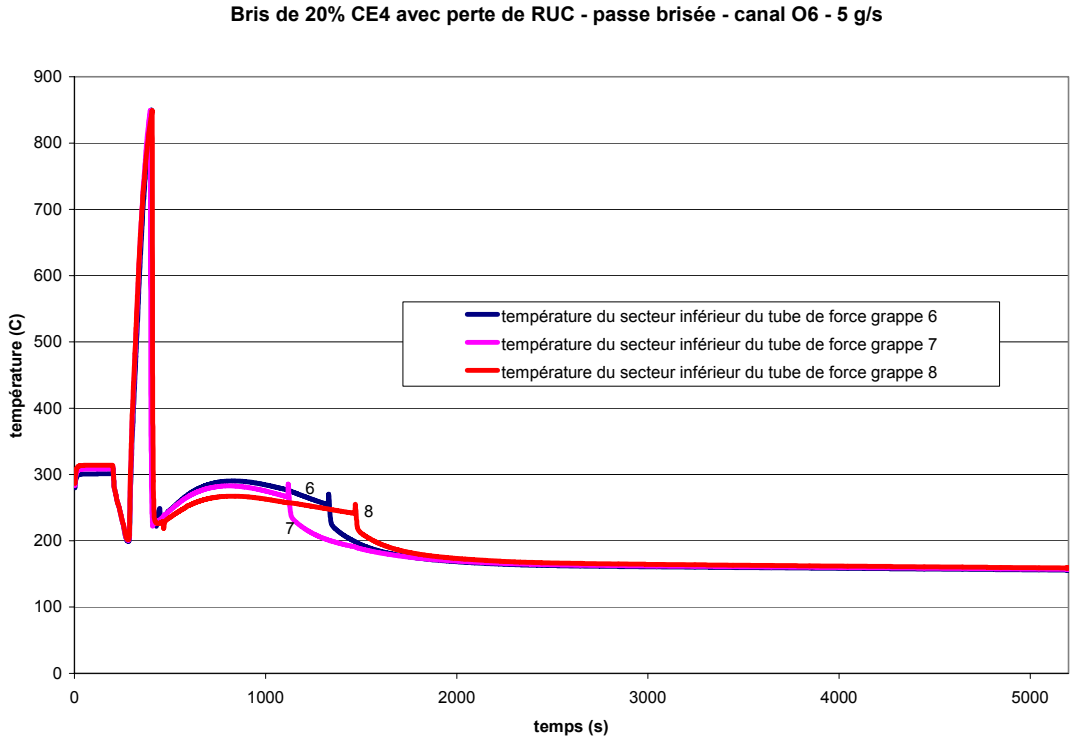

Figure 9 Pressure tube bottom sector temperatures – channel O6 – 5 g/s

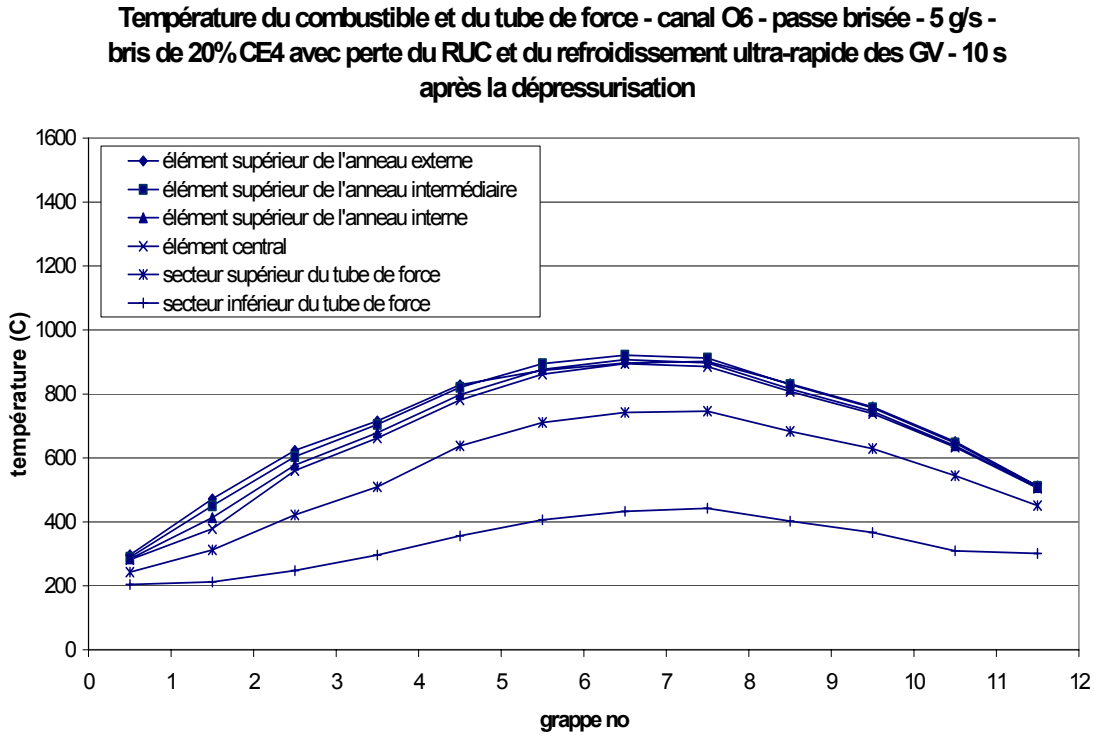

Figure 10 Axial distribution of the pressure tube and element temperatures – channel O6 – broken pass – 5 g/s- 10 s after the blowdown

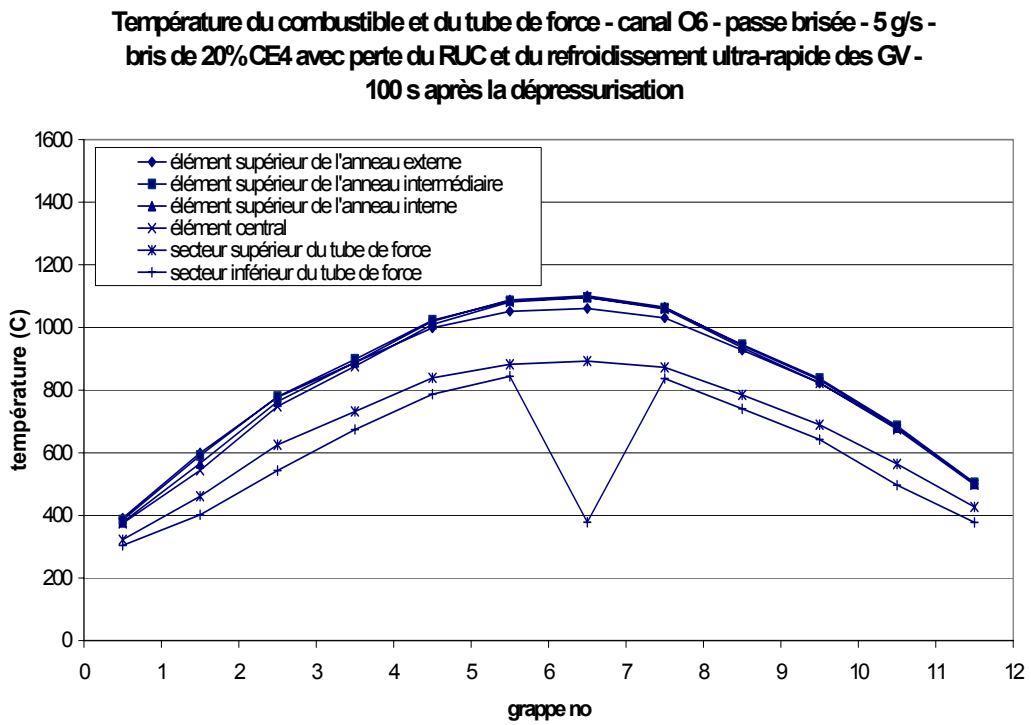

Figure 11 Axial distribution of the pressure tube and element temperatures – channel O6 – broken pass – 5 g/s- 100 s after the blowdown

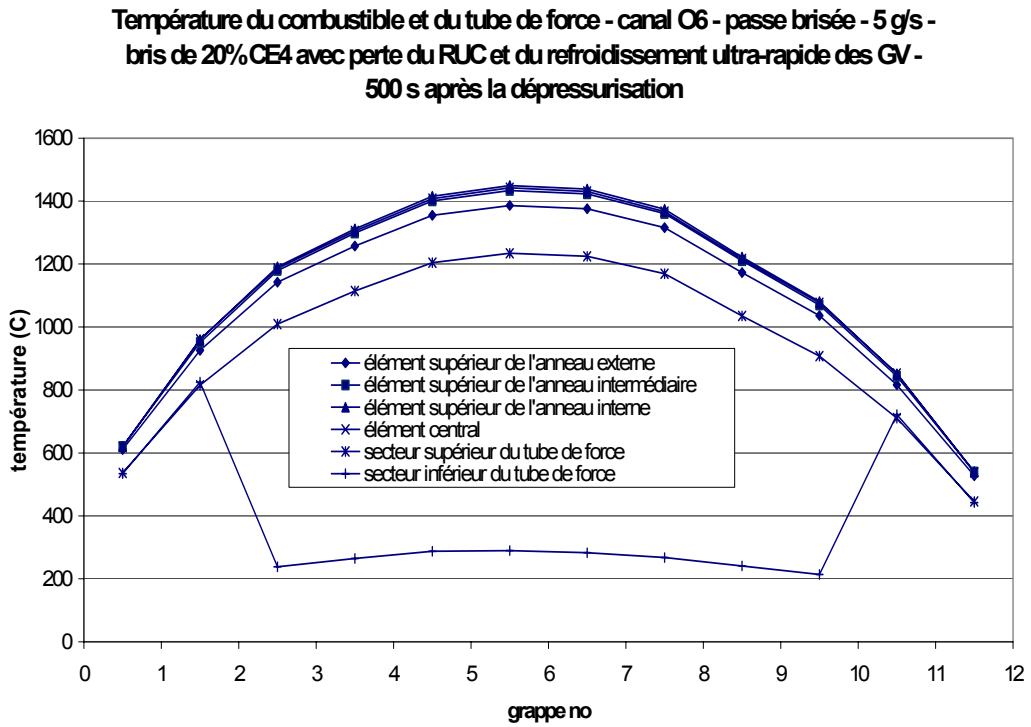

Figure 12 Axial distribution of the pressure tube and element temperatures – channel O6 – broken pass – 5 g/s- 500 s after the blowdown

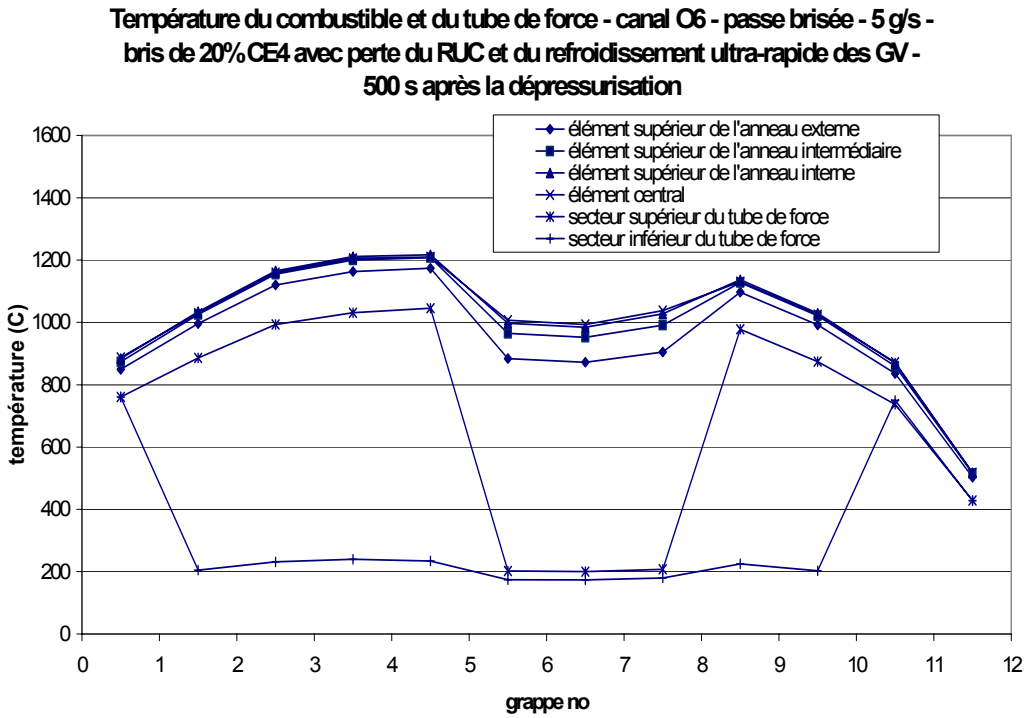

Figure 13 Axial distribution of the pressure tube and element temperatures – channel O6 – broken pass – 5 g/s- 1500 s after the blowdown

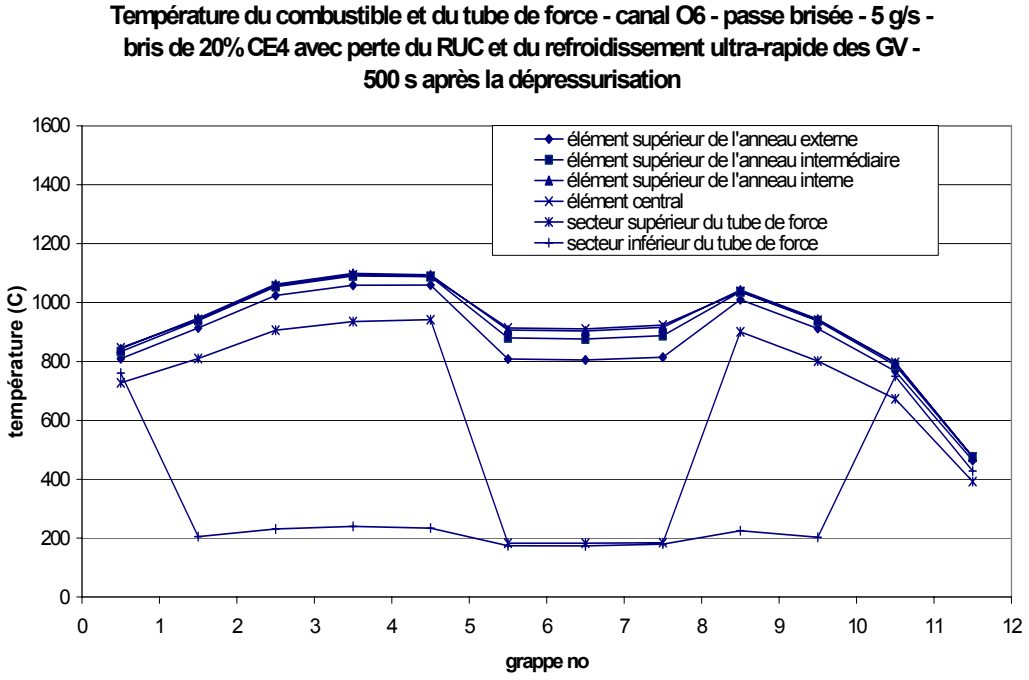

Figure 14 Axial distribution of the pressure tube and element temperatures – channel O6 – broken pass – 5 g/s- 3000 s after the blowdown

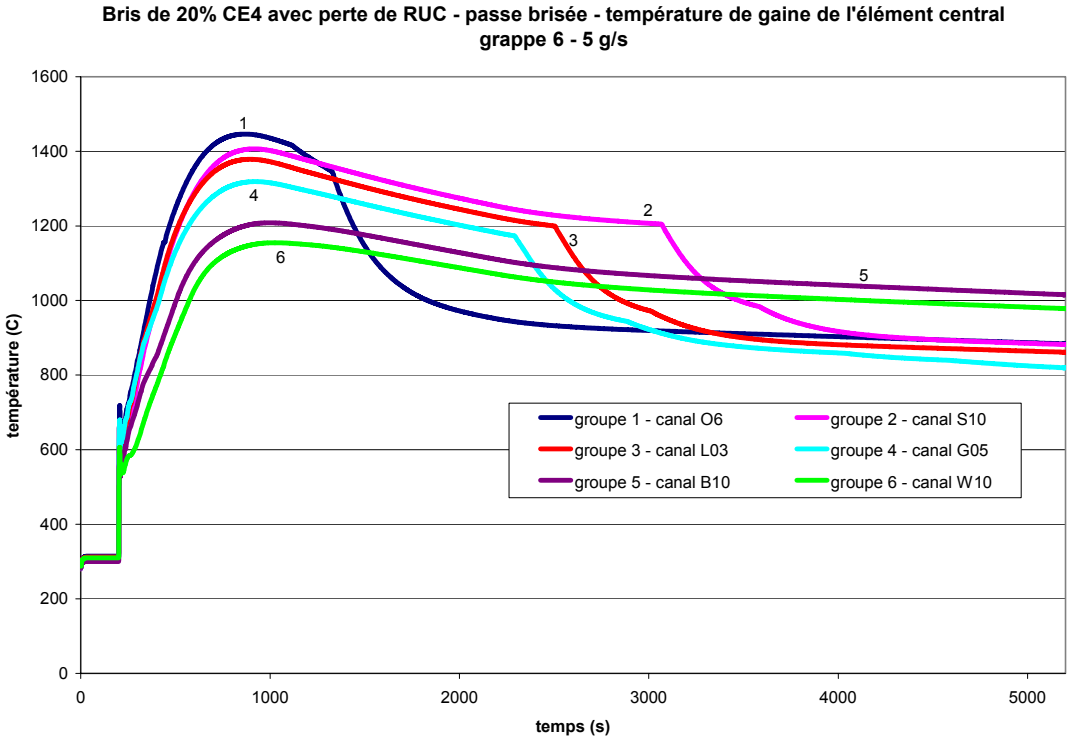

Figure 15 Central element sheath temperature – bundle 6 – comparison between channels – broken pass – 5 g/s

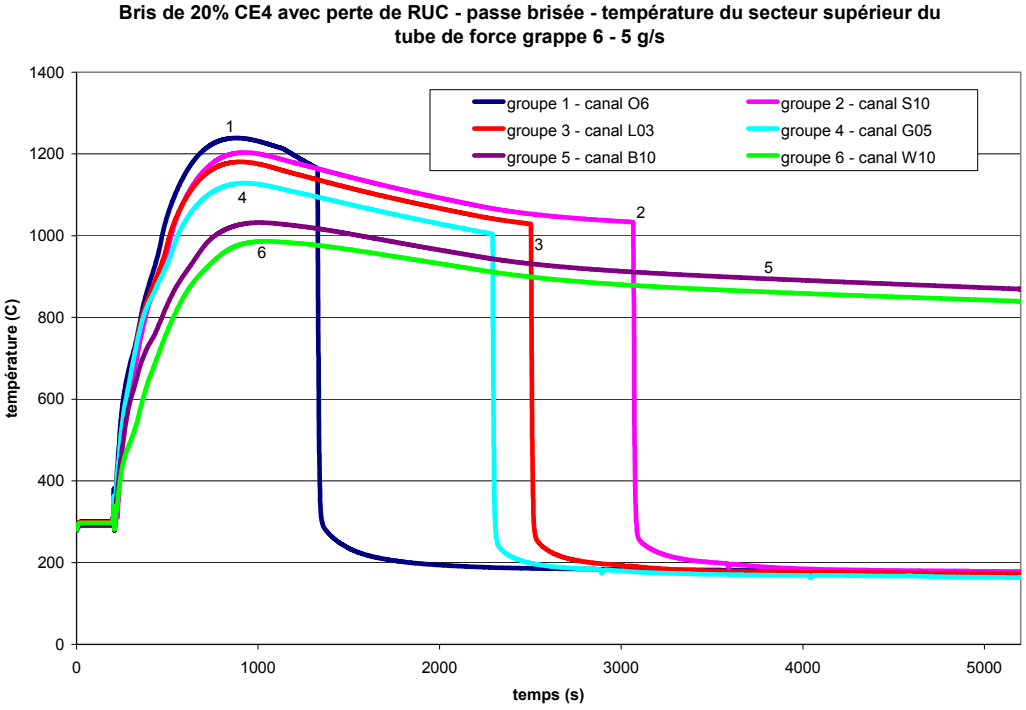

Figure 16 Pressure tube temperature – bundle 6 – comparison between channels – broken pass – 5 g/s

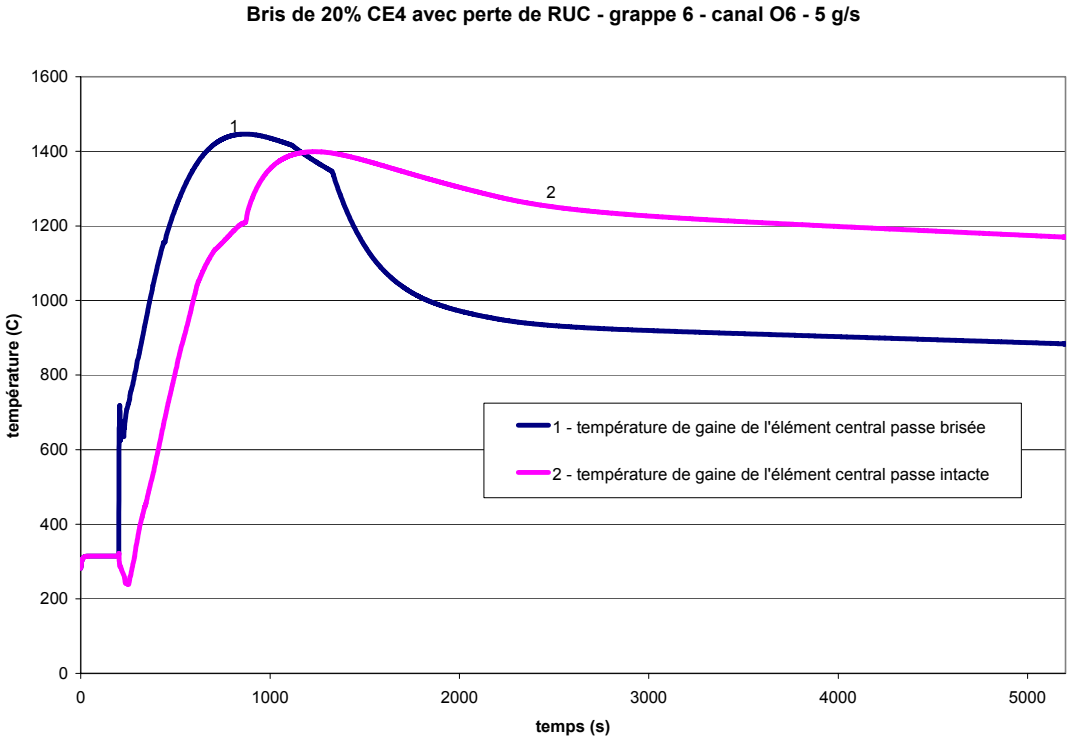

Figure 17 Comparison between the central element sheath temperatures of bundle 6 channel O6 of both passes

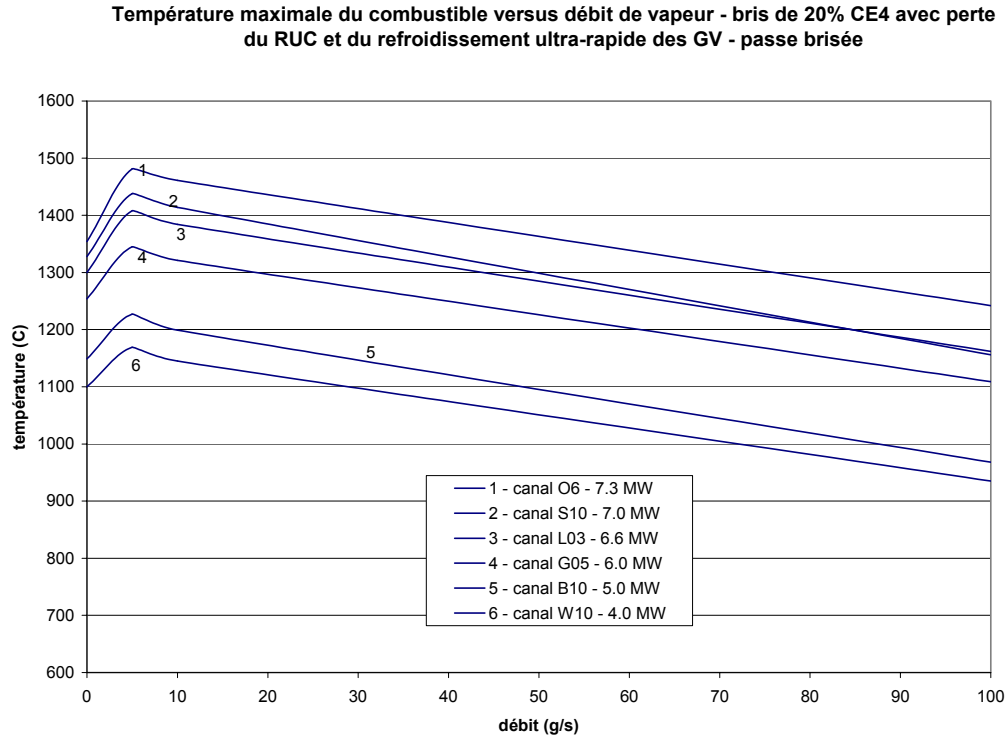

Figure 18 maximum fuel temperatures versus steam flowrate – broken pass

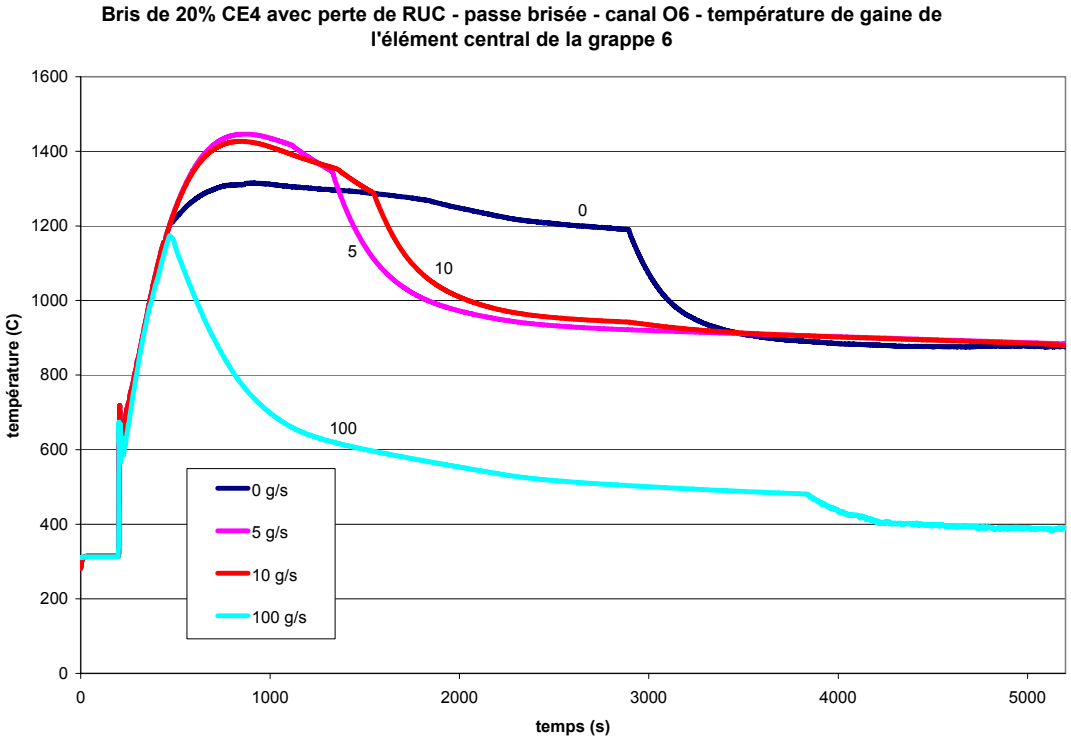

Figure 19 Comparison between the central element sheath temperatures of bundle 6 channel O6 for different constant steam flowrate

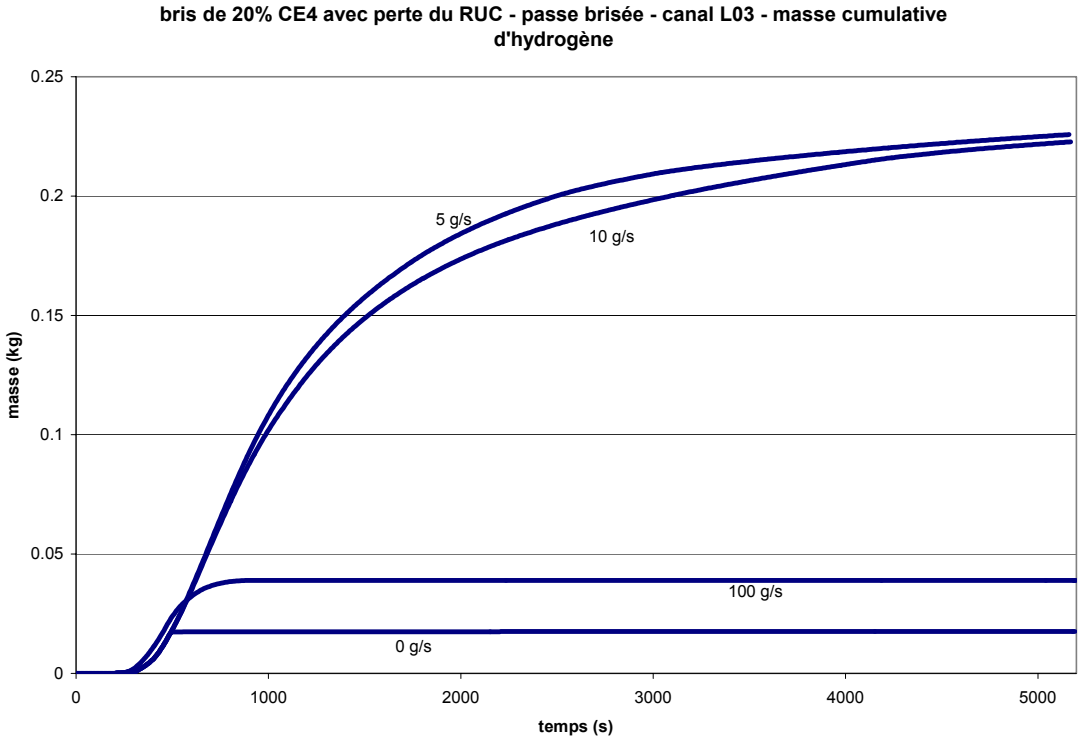

Figure 20 Comparison of the cumulative hydrogen mass produced for different steam flowrate in channel L03.

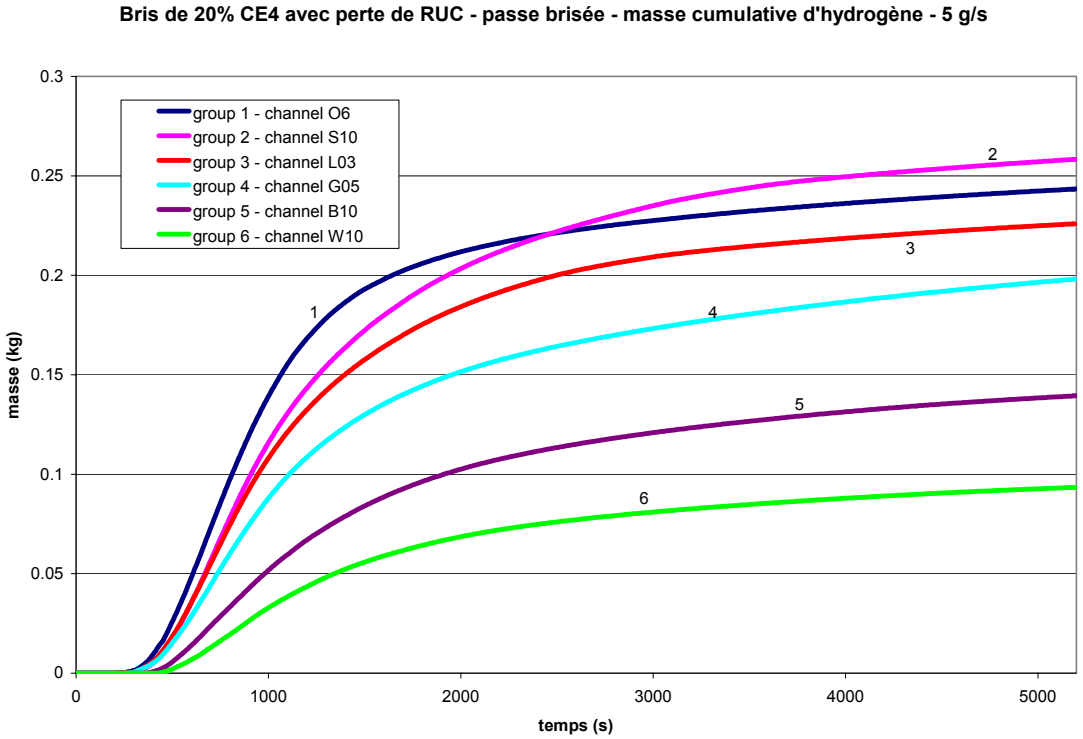

Figure 21 Hydrogen production by channel in the broken pass

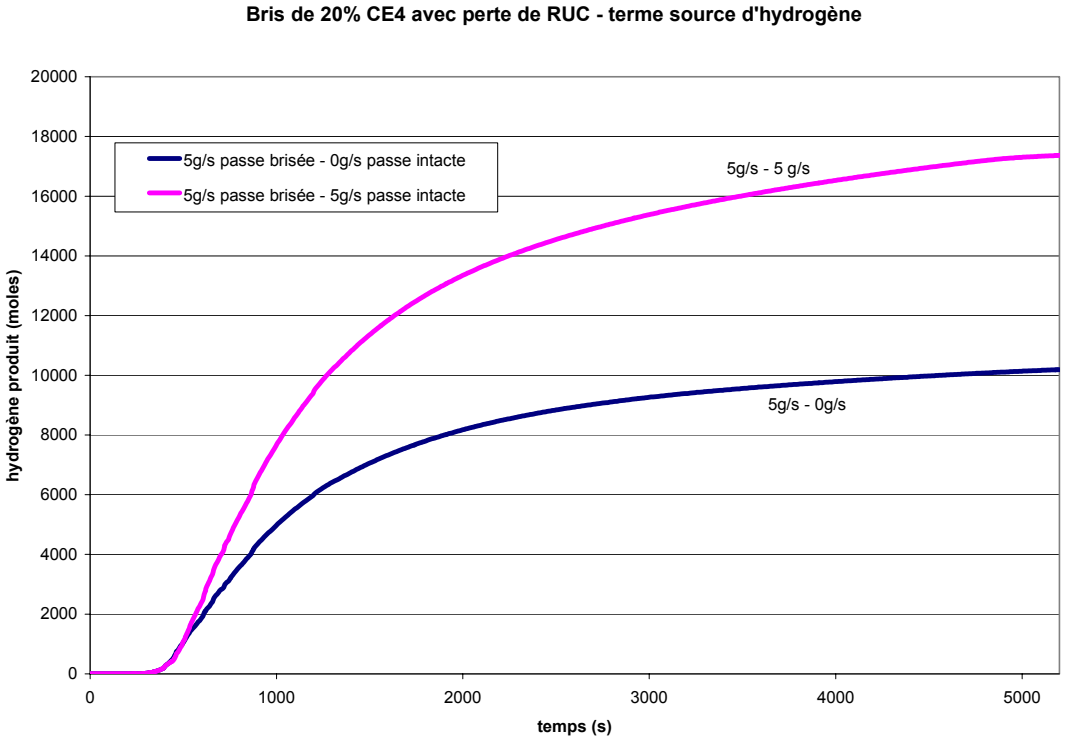

Figure 22 Hydrogen source term